Available online at www.sciencedirect.com
SCIENCE DIRECT®
Journal of Chromatography A, 998 (2003) 1–20
JOURNAL OF CHROMATOGRAPHY A
www.elsevier.com/locate/chroma

Review

Capillary zone electrophoresis of natural organic matter

Philippe Schmitt-Kopplin[a,*], Jens Junkers[b]

[a]*GSF—Forschungszentrum für Umwelt und Gesundheit, Institute for Ecological Chemistry, Ingolstädter Landstrasse 1, D-85764 Neuherberg, Germany*

[b]*GSF—Forschungszentrum für Umwelt und Gesundheit, Institute for Soil Ecology, Ingolstädter Landstrasse 1, D-85764 Neuherberg, Germany*

Received 25 October 2002; received in revised form 31 March 2003; accepted 7 April 2003

Abstract

This paper presents an in-depth look at the use of capillary electrophoretic (CE) techniques for the fingerprinting and characterization of humic substances and natural organic matter. These materials are highly heterogeneous in structure and show all characteristics of mixtures unliked in analytical chemistry. The electrophoretic approach, however, allows the determination of mobility distributions in different solution conditions, representative of the effective charge and size distribution status of the components present. A tabulated review covers over 50 references on the subject and highlights the possibilities and problems encountered in the analysis of such polydisperse materials with CE methods. In a second part of the article the consequences of experimental and buffer parameters on the behavior of humic materials in CE are presented.

Keywords: Reviews; Natural organic matter; Fulvic acids; Humic acids; Humic substances

Contents

*Corresponding author. Fax: +49-89-3487-3358.
E-mail address: schmitt-kopplin@gsf.de (P. Schmitt-Kopplin).

0021-9673/03/$ – see front matter
doi:10.1016/S0021-9673(03)00636-8

1. Introduction

Dissolved humic materials (DHMs) are the main constituents of the natural organic matter (NOM) pool in surface (fresh and marine waters), ground and soil pore waters, have colloidal properties [1] and commonly impart a yellowish–brown color to the water system. The concentration of NOM is traditionally measured based on the total dissolved organic carbon (DOC) content of the component molecules. Despite their different origins, which are responsible for their main structural characteristics, the various NOM types all constitute refractory products of chemical and biological degradation and condensation reactions of plant or animal residues and play a crucial role in many biogeochemical processes. Humic substances (HSs) are complex *heterogeneous* and *polydisperse* mixtures of non-stoichiometric composition. They can be seen in the diagenetic scale as a transformation product from animal and plant debris towards carbon dioxide and fossil fuel [2]. These reactions include both condensation and degradation in constant dynamic equilibrium. Degradation includes abiotic (photodegradation [3], hydrolysis) and biotic (microbial [4]) pathways. HSs can be generally characterized as being rich in oxygen-containing functional groups, notably carboxylic moieties, phenolic and aliphatic hydroxyl, and carbonyl in ketones and quinones. They are defined according to function rather than to structure. Isolation methods (chemical and physical fractionation procedures) of humic substances from various environmental matrices are suggested, e.g., by the International Humic Substances Society (IHSS). Compared to the operationally defined fulvic acids (FAs—soluble in both alkali and acid solutions), the humic acids (HAs—soluble in alkali, insoluble in acid solutions) are of higher molecular mass and lower total acidity. HSs affect natural processes such as soil weathering, buffering and fertility [5], pH and alkalinity of natural waters, and trace metal chemistry [6]. Their anthropogenic impacts includes bioavailability [7], degradation [8] and transport of organic chemicals, formation of disinfection by-products during water treatment, and heterotrophic production in blackwater ecosystems. Soil, aquatic and marine HSs are ubiquitous and important contributors to the global cycles of the elements C, N, P and S in the bio- and geosphere. Soil humic substances generally differ from freshwater humic substances in their elemental and functional group composition [9]. Soil HSs are typically of higher molecular mass, lower carboxylic and higher phenolic content, and exhibit higher ratios of extractable humic to fulvic acids [10]. Freshwater humic substances contain stronger acidic functions due to the presence of keto acid and aromatic carboxyl-group structures [11,12]. Marine humic substances lack lignin constituents and are of rather aliphatic and peptide origin coming from other than vascular (land) organisms plants [9,13]. Colloidal materials are only defined by their size, being sized between 1 nm and 1 μm, and their stability is largely dependent on the solution chemistry: ionic strength, pH, number of particles, size [14]. Despite these structural differences, major characteristics that affect HS reactivity in environmental compartments are their size and charge distribution, which in turn govern their hydrophilic/hydrophobic balance [15].

Capillary electrophoresis (CE) combines the unique possibility to separate and detect natural organic matter in aqueous solution within a wide pH range, i.e., close to environmental conditions, and to obtain information on their charge density (electrophoretic mobility being governed by charge and size).

The aim of this paper is to give an in-depth overview of the use of CE in the characterization of NOM and to look at different possible pitfalls and artifacts that could come either (i) from the instrumental setup or (ii) from separation buffer solution chemistry.

2. State-of-the art in CE characterization of humic substances and natural organic matter

Neihof and Loeb [16] already reported the first electrophoretic measurements on particulate and dissolved organic matter from seawater by means of the microelectrophoresis technique at the beginning of the 1970s. These early studies reported on the organic–mineral interactions through changes in surface charge of the particulate matter in different water salinity [17]. The method was further developed and adapted by Hunter [18] to measure the pH-dependent electrophoretic mobility of sea water organic coated minerals and the importance of COOH and OH groups for their binding to different metal ions.

2.1. Tabulated review on the use of capillary electrophoresis with humic substances and natural organic matter

Only a small number of applications of CE for the characterization of humic substances and natural organic matter can be found in the literature; most of the used techniques are capillary zone electrophoresis (CZE), capillary gel electrophoresis (CGE) and capillary isoelectric focusing (cIEF). Many authors attempted to use the method to investigate their samples but avoided its further use due to the difficulties in interpreting the obtained electrophoretic patterns. The references found by the end of 2002 are summarized in Table 1, including important instrument parameters, buffer systems and sample descriptions.

2.2. Comments on major problems in the use of CE methods to characterize natural organic matter

The difficulties in the interpretations of the obtained signals of humic substances with any analytical approach come from the high polydispersity in structure of these materials. Humic substances are operationally defined and consist of a mixture of constituents having a wide hydrophobic/hydrophilic range. They behave as molecules and/or colloids as a function of their own concentration in the medium and the solution's properties (ionic strength, pH) [75]. All these properties combined make a comparison of results difficult and a normalization/standardization of experimental conditions necessary.

With these problems in mind a few comments can be made on the approaches found in the literature.

(i) Fingerprinting the humic samples was the main aim of the listed papers. The methods delivering the highest number of peaks in the electropherograms were often considered to be the best. However, many authors omitted to mention that a number of these peaks can be system peaks which are only due to the buffer (for example presence of spikes due to unfiltered buffer solutions).

(ii) It is clear that artifacts caused by buffer interaction can lead to an increase in the number of reproducible signals, but the interpretation of these signals is impossible without a systematic approach. If the comparison of samples is the goal, these buffers may even be ideal, but they become a problem when interpreting the data in relation to the size and charge of native samples. Possible artifacts due to interaction with phosphate or borate ions were already described in an early paper [37] but did not catch the attention of many authors.

(iii) Promising attempts and systematic approaches to measure metal–humic interactions with CE techniques where rapidly abandoned because, again, of the problems in the interpretation of the complex electropherograms. These problems, however, were inevitably nearly always related to the choice of the separation buffer: for example, borate ions compete with the same humic binding sites as metals.

(iv) When trying to correlate the electrophoretic behavior of humic substances with their structural characteristics (as, for example, time versus molecular size), the basic principles of CE were often ignored; i.e., correlations were often done with time parameters in different electroosmotic flow (EOF) conditions.

(v) The use of very specific samples without including standard materials (i.e., from the IHSS) makes any comparison between authors even more difficult.

(vi) Unrealistic buffer systems (pH lower than 3, zwitterionic or cationic buffers) were used with humic acids, yielding peaks (system peaks?) that can either be representative of the sample or of displaced buffer zones due to the interaction. How can such

Table 1
Exhaustive list of publications dealing with the use of capillary electrophoresis to characterize humic substances

Ref.	Instrument	Method	Detection	Capillary	Injection time, volume	Buffer	Samples	Goal of the study
[19]	Applied Biosystems 270A-HT	CZE CGE	UV–Vis 400 nm	Fused-silica, uncoated, 55 (30 t.d.) cm×75 μm I.D.	3 s	Tris–phosphate 50 m*M*, pH 8.3, PEG 0–50 g/l	Peat HS	Fingerprinting of peats
[20]	Thermo Bioanalysis Spectraphoresis 2000	CZE	UV–Vis 220 nm	Fused-silica, uncoated, 43.5 (35.5 t.d.) cm×75 μm I.D.	30 s	HCl–DL-alanine 60 m*M*, pH 3.2	Soil, compost HAs	Fingerprinting
[21]	Bio-Rad BioFocus 3000	CZE	UV–Vis 254 nm	Fused-silica, uncoated, 24 (–) cm×25 μm I.D.	1 nl	100 m*M* phosphate, pH 8.5, Normex borate, pH 9.0	Peat HAs, size fractioned	Fingerprinting
[22]	Bio-Rad BioFocus 3000	CZE	UV–Vis 254 nm	Fused-silica, uncoated, – (24) cm×25 μm I.D.	1–30 nl	Borate 50 m*M*, pH 9.7, 8.9, 8.15, phosphate 50 m*M*, pH 7.1, citrate–HCl 50 m*M*, pH 6.25, 2.3	Peat FAs	Fingerprinting
[23]	Waters Quanta 4000	CZE	UV–Vis 254 nm	Fused-silica, uncoated, 78.5 (71 t.d.) cm×75 μm I.D.	n.i.	Borate 79.2 m*M*, pH 8.3	Water FAs, lignin, M_r-standards	Evaluation of CZE for fingerprinting
[24]	Applied Biosystems 270A	CZE CGE	UV–Vis 360 nm	Fused-silica, uncoated, 55 (30 t.d.) cm×75 μm I.D., polyacrylamide coated, 55 (30 t.d.)×50 μm I.D.	2 s	Tris–phosphate 50 m*M*, pH 8.3, Tris–phosphate 25 m*M* +PEG 4000, 0–15% (w/v)	Soil, compost HSs	behavior of HSs in PEG (EOF, buffer, pH effects)
[25]	Applied Biosystems 270A	CZE CGE	UV–Vis 360 nm	Fused-silica, uncoated, 55 (30 t.d.) cm×75 μm I.D., polyacrylamide coated, 55 (30 t.d.)×50 μm I.D.	2 s	Tris–phosphate 100 m*M*, 50 m*M*, pH 6.3, 10.3, Tris–phosphate 50 m*M* +PEG 4000, pH 8.3	Soil, peat HSs	pH, molecular size effects on CE
[26]	n.d.	CZE CGE	UV–Vis 400 nm	Fused-silica, DB-Wax coated, 55 (30 t.d.) cm×100 I.D.	1 s	Tris–phosphate 50 m*M*, pH 8.3, +PEG 4000/20 000	Soil HSs, size fractioned	Size, charge effects in CGE
[27]	Applied Biosystems 270A-HT	CZE CGE	UV–Vis 210 nm 360 nm	Fused-silica, uncoated, 55 (30 t.d.) cm×75 μm I.D., polyether coated, 55 (30 t.d.)/100(75 t.d.)×100 μm I.D.	3 s	Tris–phosphate 50 m*M*, pH 8.3 +PEG/PVA	Peat HSs, size fractioned HSs	behavior in CGE of different HSs and different PEG concentrations
[28]	Applied Biosystems 270A-HT	CZE CGE	UV–Vis 360 nm	Fused-silica, uncoated, 55 (30 t.d.) cm×75 μm I.D., DB-Wax coated, 55 (30 t.d.)×75 μm I.D.	2 s	Tris–phosphate 50 m*M*, pH 8.3 +PEG	Soil HSs, size fractioned	Behavior in CGE
[29]	Applied Biosystems 270A-HT	CZE CGE	UV–Vis 360 nm	Fused-silica, uncoated, 55 (30 t.d.) cm×75 μm I.D., polyacrylamide coated, 55 (30 t.d.)×50 μm I.D., DB-Wax coated, 55 (30 t.d.) cm×100 i.d	3 s	Tris–phosphate concentration range 25–75 m*M*, pH range 6.3–10.3, different PEG concentrations	Soil, peat HSs, size fractioned	behavior of HSs in PEG (EOF, buffer, pH effects)
[30]	Dionex	CZE CGE	UV–Vis 220 nm	Fused-silica, uncoated, 55 (50 t.d.) cm×75 μm I.D., polyacrylamide coated, 50 (45 t.d.) cm×75 μm	10 s	Acetate, L-alanine, borate, MES, Tris, CAPS, CHES concentration range 5–20 m*M*, pH 3.17–10.40	Water HAs, FAs	Attempt in comparison of different electrophoretic methods

[31]	Agilent Technologies	CZE	UV–Vis 254 nm	Fused-silica, uncoated, 80 (75 t.d.) cm×75 μm I.D.	5 s	Phosphate 25 m*M*, 5 *M* urea, 10% acetonitrile, 5% dimethylsulfoxide	Lake NOM	Fingerprinting, principal component analysis
[32]	Thermo Bioanalysis 2000	CZE	UV–Vis scan 190–600 nm	Fused-silica, uncoated, 43.5 (35.5 t.d.) cm×75 μm I.D.	15/20 s	Borate, various HCl–amino acid mixtures	Coal HAs, Fluka HAs	Fingerprinting of HAs
[33]	Thermo Bioanalysis Spectraphoresis 2000	CZE	UV–Vis scan 190–700 nm	Fused-silica, uncoated, 43.5 (35.5 t.d.) cm×75 μm I.D., polyacrylamide, 43.5 (35.5 t.d.) cm×75 μm I.D.	18 s	Rimantadine hydrochloride 20 m*M*, pH 3.0–6.0	Coal HAs, Fluka HAs	Fingerprinting and trials in optimizing metal interactions
[34]	Thermo Bioanalysis Spectraphoresis 2000	CZE	UV–Vis scan 190–700 nm	Fused-silica, uncoated, 43.5 (35.5 t.d.) cm×75 μm I.D., polyacrylamide, 43.6 (35.6 t.d.) cm×75 μm I.D.	18–20 s	HCl 8 m*M*/l, +L-alanine 60 m*M*/l, pH 3.17, rimantadine HCl 20 m*M*, pH 3.4, borate 100 m*M*, pH 3.15	n.i.	Fingerprinting/interpretations as aggregation and adsorption of HAs on capillary not taking account of the EOF
[35]	Beckman PACE 5500	CZE	UV–Vis 210 nm	Fused-silica, uncoated, 47 (40.3 t.d.) cm×75 μm I.D.	22 s	Borate 50 m*M*, pH 9	IHSS standards (peat, leonardite), Fluka soil, peat HAs	Fingerprinting, comparison attempts of the fingerprints to offline MS
[36]	Beckman PACE 5500	CZE	UV–Vis 210 nm	Fused-silica, uncoated, 47 (40.3 t.d.) cm×75 μm I.D.	20 s	Tris–borate 90 m*M*, pH 8.3	Soil organic matter, IHSS soil HAs,Chemapex coal HAs	Fingerprinting
[37]	Beckman PACE 2100	CZE CGE	UV–Vis 254 nm	Fused-silica, uncoated, 57 (50 t.d.) cm×75 μm I.D.	5–10 s	Acetate 50 m*M*, pH 4.95, borate 90 m*M*, pH 8.3, citrate pH 3.2–8.3	IHSS (soil, water), soil, water, ground water HSs	First trial of CZE, CGE with HSs effect of borate buffers effects of pH, voltage
[38]	Thermo Bioanalysis Spectraphoresis 2000	CZE	UV–Vis scan 192–700 nm	Fused-silica, uncoated, 43.6 (35.6 t.d.) cm×75 μm I.D.	18 s	Borate 350 m*M*, pH 3.15	IHSS standards (peat, leonardite, soil)	Fingerprinting, attempt in comparison to offline MS detection
[39,40]	Beckman PACE 2100	CZE	UV–Vis 200/214 nm	Fused-silica, uncoated, 37/47/57 (–) cm×100 μm	10 s	Acetate, MES, malonate, BES, AMPSO, carbonate, 5–120 m*M*, pH 3.9–10.9	IHSS standards (soil, peat, water)	Relation mobility to charge and size
[41]	Spisská Nová Ves isotachophoretic analyser	ITP CZE	Conductivity detection	Fused-silica/PTFE (130–180 t.d.) mm×300 μm I.D.	200 nl sample loop	PEG–DC–Bis–Tris propane–PVP	Drinking water pH 3.5; succinate–Bis–Tris propane–PVP, pH 3.55	aqueous soil extracts
[42]	Spisská Nová Ves isotachophoretic analyser	ITP	UV–Vis 405 nm	n.i.	n.i.	n.i.	Commercial, water peatbog, water HSs	Fingerprinting
[43]	Waters Quanta 4000	CZE	UV–Vis 214 nm	Fused-silica, uncoated, 50 (42 t.d.) cm×75 μm I.D.	30 s	Borate pH 9.00, phosphate pH 9.10	Fog HSs, Aldrich, peat and water HAs	Fingerprinting of fog HSs

Table 1. Continued

Ref.	Instrument	Method	Detection	Capillary	Injection time, volume	Buffer	Samples	Goal of the study
[44]	Agilent Technologies	CZE	UV–Vis 214 nm	Fused-silica, uncoated, 70 (63 t.d.) cm×50 μm I.D.	20 s	Borate, pH 9.3	Soil, peat, compost HAs, Aldrich HAs	Fingerprinting HAs of different origins /borate not recognized
[45]	Beckman PACE 5510	CZE	UV–Vis DAD	Fused-silica, uncoated, 57 (50 t.d.) cm×75 μm I.D.	20/30 s	Different borate buffers, pH 4.5–9.0	Water FAs	Metal–FA interactions
[46]	Beckman PACE 5510	CZE	UV–Vis scan 190–600 nm LIF 488 ex, 520 em	Fused-silica, uncoated, 57 (50 t.d.) cm×75 μm I.D.	2/20 s	Borate 10 m*M*, pH 9	Soil HAs, water FAs	Fingerprinting
[47]	Beckman PACE 5500	CZE	UV–Vis DAD 210 nm	Fused-silica, uncoated, 37 (30.5 t.d.) cm×75 μm I.D.	20 s	Borate 90 m*M*, pH 8.4, addition of Tris and EDTA in various concentrations	IHSS standard HAs (soil, leonardite), soil peat and coal HSs	Fingerprinting HAs of different origin; optimizing buffer composition
[48]	Beckman PACE 5500	CZE	DAD LIF 488 ex, 520em	Fused-silica, uncoated, 57 (50 t.d.) cm×75 μm I.D.	15 s	Phosphate–borate systems pH 9.3	Lake NOM	CE characterization of RP-HPLC fractions using borate complexation
[49]	Beckman PACE 5500	CZE	UV–Vis 210 nm	Fused-silica, uncoated, 47 (40.3 t.d.) cm×75 μm I.D.	22 s	Borate 50 m*M*, pH 9	IHSS standards (peat, leonardite), Chemapex HAs, Aldrich, coal HAs	Fingerprinting and attempts in comparison to offline MS
[50]	Beckman PACE 5500	CZE	UV–Vis 210 nm	Fused-silica, epoxy-coated, 47 (40.3 t.d.) cm×75 μm I.D.	22 s	Borate 50 m*M*, pH 9.6, CDs, methanol, oligosaccharides	Coal HAs, IHSS peat HAs, Fluka HAs	Fingerprinting
[51]	Beckman PACE 5500	CZE	UV–Vis 210 nm	Fused-silica, uncoated, 47 (40.3 t.d.) cm×75 μm I.D.	20 s	Tris–borate 90 m*M*, pH 8.3	Commercial HAs	Fingerprinting
[52]	Beckman PACE 2050	CZE	UV–Vis 214 nm	Fused-silica, uncoated, 50 (?) cm×75 μm I.D.	70 nl	Borate 6 m*M* +phosphate 3 m*M*, pH 8.9	Soil HSs, river HSs, commercial HAs	Fingerprinting
[53]	Beckman PACE 2050	CZE	UV–Vis 214 nm	Fused-silica, uncoated, 40 (?) cm×75 μm I.D.	70 nl	Borate 6 m*M*+phosphate 3 m*M*, pH 8.9	Synthetic HAs, Fluka HAs	Two HAs+interaction with uranium—but in borate buffers
[54]	Applied Biosystemss 270A	CZE	UV–Vis 215 nm	Fused-silica, uncoated, 72 (50 t.d.) cm×75 μm I.D.	12 s	HCl 8 m*M*/l+L-alanine 59.8 m*M*/l, pH 3.17	Fluka HAs, Soil HAs	Attempts to estimate HA contents in soil
[55]	Applied Biosystems 270A	CZE	UV–Vis scan 190–700 nm	Fused-silica, uncoated, 72 (?) cm×50 μm I.D.	12 s	12 HCl–amino acid mixtures, acidic pHs	Commercial HAs	Attempts to estimate HA contents in soil

[56]	Applied Biosystems 270A	CZE	UV–Vis 215 nm	Fused-silica, uncoated, 72 (? t.d.) cm×50 μm I.D.	12 s	L-Alanine+HCl, pH 3.17	Soil HAs, Fluka HAs	Attempts to estimate HAs in soil /radiocaesium mobility
[57]	Applied Biosystems 270A	CZE	UV–Vis 215 nm	Fused-silica, uncoated, 72 (50 t.d.) cm×50 μm I.D.	12 s	L-Alanine+HCl, pH 3.2	Soil HAs, Fluka HAs	CE of HAs separated by ultrafiltration
[58]	Beckman PACE 2050	CZE cIEF CGE	UV–Vis 214/230/254 nm	Fused-silica, uncoated, 57 (50 t.d.) cm×75 μm I.D.	n.i.	Acetate 50 m*M*, pH 4.5, citrate pH 2–8, borate 50 m*M*, pH 8.3	Soil HAs, FAs	Application of different CE methods
[59]	Beckman PACE 2050	CZE	UV–Vis 214/230 nm	Fused-silica, uncoated, 57 (50 t.d.) cm×75 μm I.D.	10–20 s	Acetate 50 m*M*, pH 4.65	Soil HAs, FAs	Atrazine photolysis, only part CE
[60]	Beckman PACE 2050	CZE	UV–Vis 254 nm	Fused-silica, uncoated, 57 (50 t.d.) cm×75 μm I.D.	5–10 s	Acetate pH 4.95, borate pH 9.3	Soil HAs, FAs	Mobility changes during flocculation with Fe and Cu, charge eutrallization
[61]	Beckman PACE 2050	ACE	UV–Vis 230 nm	Fused-silica, uncoated, 57 (50 t.d.) cm×75 μm I.D.	10 s	Acetate 50 m*M*, pH 4.6 HSs as micellar phase	Soil, water, IHSS Aldrich HAs, FAs,	Binding of *s*-triiazines to HSs structure–reactivity effects
[62]	Beckman PACE 2050/5000	cIEF CZE	UV–Vis	Fused-silica, uncoated, 57 (50 t.d.) cm×75 μm I.D.; eCAP 50 μm×20 cm t.d.	n.i.	Acetate 50 m*M*, pH 5.1, borate 20 m*M*, pH 8.3; ampholytes 3–10+cIEF gels (Beckman cIEF Kit)	Soil, water HAs, FAs, IHSS water HAs, FAs	cIEF for characterization of HSs from different sources, compared to classical liquid IEF, pH dependent CZE of IEF fractions, borate effect
[63]	Beckman PACE 2050, Bio-Rad BioFocus 3000	CZE	UV–Vis 254 nm	Fused-silica, uncoated, 57 (50 t.d.) cm×75 μm I.D.	5/10 s	Acetate pH 4.95, phosphate pH 6.3, borate pH 8.3	Soil, water HAs, FAs, IHSS standards soil water HAs FAs	Fingerprinting/characterization borate interactions
[64]	Beckman PACE 2050, Bio-Rad BioFocus 3000	CZE	UV–Vis 254 nm, scan 200–360 nm	Fused-silica, uncoated, 57 (50 t.d.) cm×75 μm I.D.	5/10 s	Acetate 50 m*M*, pH 4.95, borate 40 m*M*, pH9.3, carbonate 50 m*M*, pH9.3	IHSS standards soil, water), soil HAs, FAs	Characterization, buffer effects (borate), mobility calculations

Table 1. Continued

Ref.	Instrument	Method	Detection	Capillary	Injection time, volume	Buffer	Samples	Goal of the study
[65]	Beckman PACE 2050	CZE	UV–Vis	Fused-silica, uncoated, 57 (50 t.d.) cm×75 μm I.D.	n.i.	Acetate 50 m*M*, pH 5.3	soil HAs, FAs	Soil humic photodegradation studies—CE as additional analytical tool
[66]	Beckman PACE 2050/5000	CZE	UV–Vis 254 nm	Fused-silica, uncoated, 57 (50 t.d.) cm×75 μm I.D.	5/10 s	Borate 0–160 m*M*, pH 9.1	IHSS water HAs, soil HAs	Influence of borate buffers
[67]	Beckman PACE 2050	ACE	UV–Vis 280 nm LIF ex 325 nm, em 420 nm	Fused-silica, uncoated, 57 (50 t.d.) cm×75 μm I.D.	5/10 s	Carbonate 50 m*M*/25 m*M*, pH 9.2, HSs as micellar phase	soil HAs, FAs	Analysis of the photodegradation of fluoroquinoloneswith HSs, ACE binding study
[68]	Beckman PACE 2050, Bio-Rad BioFocus 3000	CZE	UV–Vis 254 nm	Fused-silica, uncoated, 57 (50 t.d.) cm×75 μm I.D.	5/10 s	Acetate 50 m*M*, pH 4.95, borate 40 m*M*, pH 9.3, carbonate 50 m*M*, pH 9.3	IHSS standards soil water HAs FAs soil HAs, FAs, synthetic HAs, HSs	Analysis of synthetic HSs for environment/medicine applications
[69]	Beckman PACE 2050	CZE	UV–Vis 254 nm	Fused-silica, uncoated, 57 (50 t.d.) cm×75 μm I.D.	5/10 s	Acetate 50 m*M*, pH 5.05, carbonate 50 m*M*, pH 9.03/11.4	IHSS standards (soil, peat, water HSs, water NOM), soil HSs	Mobility distribution of synthetic/natural polyelectrolytes
[70]	Beckman PACE 2100, Bio-Rad BioFocus 3000	CZE IEF	UV–Vis 254 nm scan 200–360 nm	Fused-silica, uncoated, 57 (50 t.d.) cm×75 μm I.D.	5/10 s	Acetate 50 m*M*, pH 5.1, borate 40 m*M*, pH 9.0, carbonate 25 m*M*, pH 9.3, 11.4	NOM isolates (Professor Gjessing)	Characterization of nordic lake NOM pH effects, Stoke's radii
[71]	Beckman PACE 2100, Bio-Rad BioFocus 3000	CZE CGE ACE	ESI-MS UV–Vis LIF	Fused-silica, uncoated, 80 (20 t.d.) cm×75 μm I.D.	2–30 s	Ammonium acetate 20 m*M*, pH 5.1, ammonium carbonate 10 m*M*, pH 9.3, pH 11.4	IHSS standards, and soil, water, marine samples . . .	Relation between HS structure and CZE behavior, molecular and colloidal behavior of HSs and NOM
[72]	Waters Quanta 4000	CZE	UV–Vis 254 nm	Fused-silica, uncoated, 60 (52 t.d.) cm×75 μm I.D.	n.i.	Acetate pH 4/6, borate pH 8	Fluka HAs, river water	Interaction with metals
[73]	Microchip CE	Micro CZE	LIF	quartz glass, 24 mm	2 s	Tris–CHES 100 m*M*, pH 8.8	Water HAs, FAs, water DOCs	Fingerprinting of river water DOCs; developmentof microchip CE device
[74]	Beckman PACE 2100	CZE	UV–Vis 254 nm	Fused-silica, uncoated, 57 (50 t.d.) cm×75 μm I.D.	n.i.	Borate 40 m*M*, pH 8.37	Soil FAs	Photodegradation studies of soil FAs, CE one analytical tool

ITP=Isotachophoresis; ACE=affinity capillary electrophoresis; DAD=diode array detection; t.d.=to detector; PEG=poly(ethylene glycol); PVA=poly(vinyl alcohol); CAPS=3-cyclohexylamino-1-propanesulfonic acid; CHES=2-(*N*-cyclohexylamino)ethanesulfonic acid; BES=*N*,*N*-Bis(2-hydroxyethyl)-2-aminoethanesulfonic acid; AMPSO=*N*-(1,1-Dimethyl-2-hydroxyethyl)-3-amino-2-hydroxypropansulfonic acid; PVP=polyvinylpyrrolidone; CD=cyclodextrine; DOC=dissolved organic carbon.

drastic chemical conditions be used to obtain structural information (such as charge states, size, aggregation, gel formation and phase transitions) that are characteristic of HSs in non-complexing environmental conditions?

One can see the complexity of the problem when taking into account that the analytical tool used for the ''characterization'' of undefined heterogeneous materials is functionally complex itself and still under development.

3. Interpreting the humic humps

Humic substances, extracted as mixtures from soil according to their solubility in acids and bases and from surface waters according to their affinity to XAD-8 resins, are considered as relatively high-molecular-mass polyelectrolytes containing aromatic, aliphatic and heterocyclic subunits. The degree of ionization of their phenolic and carboxylic groups is governed by the CE buffer pH. In CE, fulvic acids exhibit a consistent and characteristic set of sharp peaks (phenolic acids), extending from a humic ''hump'' [37]. The average electrophoretic mobility (AEM) of these humps depends on humic structure, experimental conditions and buffer composition [76,77]. Humic acids give only the ''hump'' (sometimes multiple humps). Examples of electropherograms and their interpretation will be shown below.

3.1. A question of data representation: the mobility scale

The plot of UV-absorbance versus effective mobility (μ_{eff}) shows the Gaussian-like distribution around an AEM. This representation of the primary electrophoretic data in the μ_{eff} domain is a useful visualization of effective mobility because it takes into account the changes in electroosmotic flow that can occur from one measurement to the other (dependent on buffer chemistry—pH, ionic strength, type of buffer) [69]. An electropherogram in this new scale can be considered as a frequency distribution of individual molecules (or ''molecular associates'' in these experimental conditions) having a given effective electrophoretic mobility. From the relation between mobility with charge and size using model compounds, structural information can be derived directly from the electropherograms in mobility scale [71].

Mobility scaling always includes (i) the use of an internal standard (usually *p*-hydroxybenzoic acid—phb, or an EOF marker), (Fig. 1a), (ii) the baseline correction (Fig. 1b), (iii) the scale transformation from migration time to effective mobility and (iv) the

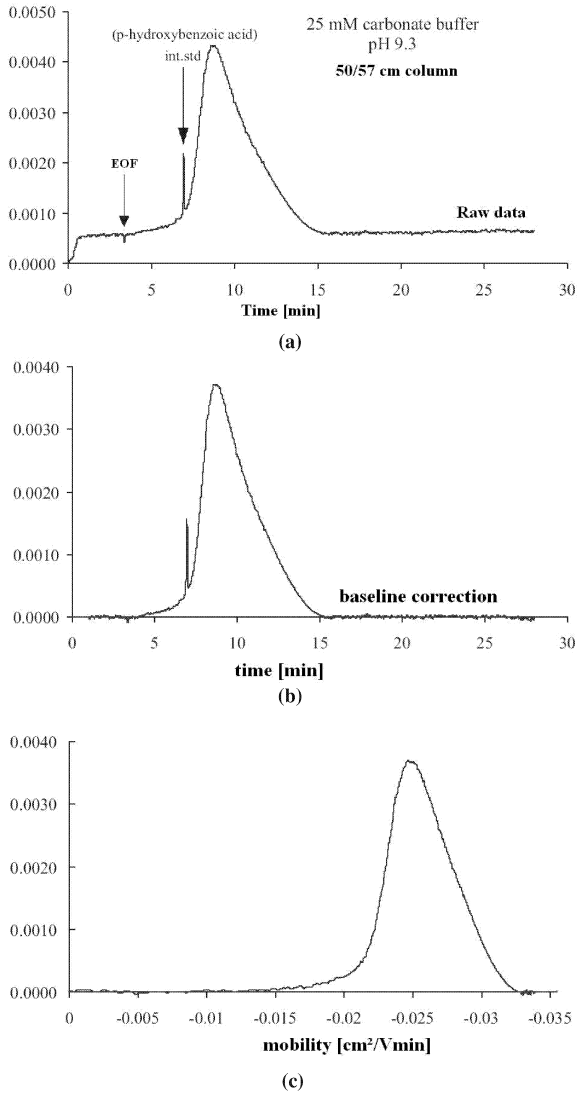

Fig. 1. (a) Raw data of SRNOM with an internal standard for this separation buffer. (b) Time-scaled data after baseline correction. (c) Converted mobility scale data using phb as internal mobility standard.

deletion of the internal standard peak (Fig. 1c). The sign of the mobility scale is negative for anions and positive for cations; to avoid confusion speaking of high mobility always implies the absolute value of the mobility.

3.2. Consequences of the mobility scale

Utilizing the mobility scale reveals tremendous effects on the qualitative and quantitative interpretation possibilities of the data when analysing single components [78,79]. Changing the time scale to mobility can have enormous effects on the electropherogram shape and the resulting interpretations when the samples are mixtures. This is illustrated in Fig. 2, with the example of Bouzule pseudogley soil fulvic acid (FA2) dissolved in 100 m*M* sodium dodecyl sulfonate (SDS) and separated in a 25 m*M* carbonate and 100 m*M* SDS buffer at pH 9.2. The data acquisition is in the time scale (between 5 and 10 data points/s). When converting to mobility scale (mobility=1/time), the electropherogram's shape is ''compressed'' and is significantly changed. More data points describe peaks in the high mobility

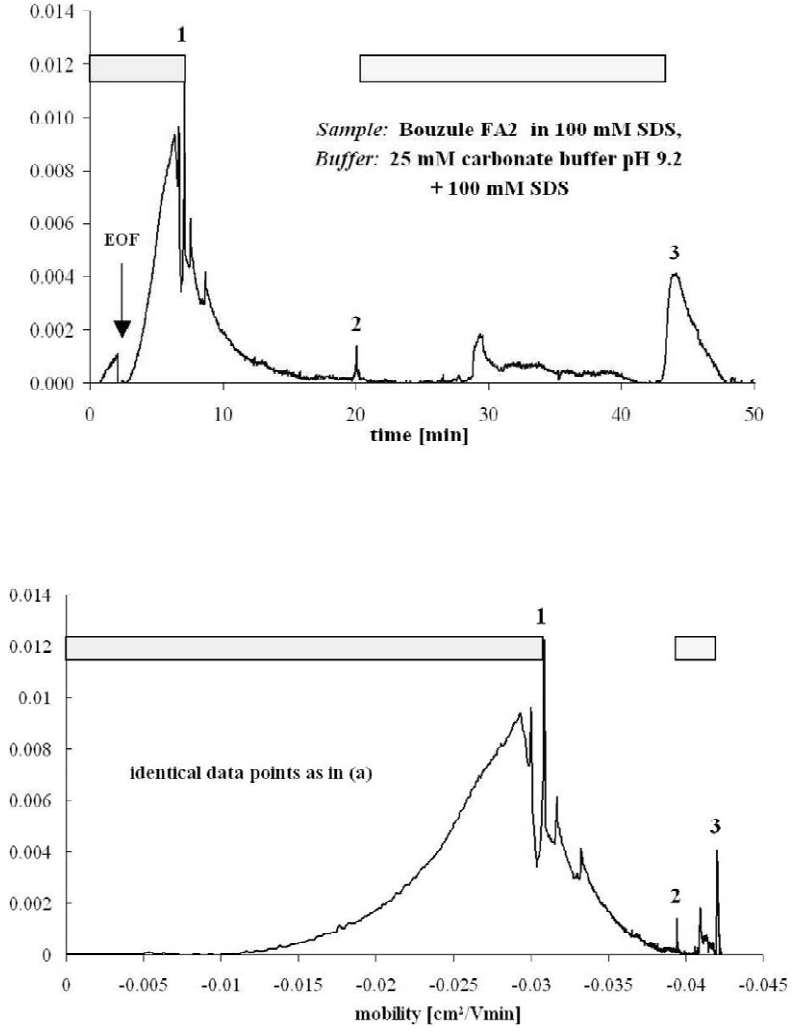

Fig. 2. Effects of scale transformation on electropherogram shape. The squared marks correspond to the same signal regions in time scale and in mobility scale between peaks 1, 2 and 3.

region than near the EOF (as a consequence, the good description of analytes migrating near the EOF should be done with a high data acquisition rate). The mobility scale is a representation of the mobility distribution in the sample and the time scale is overestimating the contribution of high mobility components. The same area in time and in mobility scale is illustrated with the boxes in the electropherograms. SDS in the sample and in the buffer significantly interacts with the fulvic acids that show individual sharp peaks out of the hump. This SDS buffer is typical for micellar electrokinetic chromatography (MEKC), and the distribution along the mobility axis is not only a function of the charge-to-size ratio, but additionally of the hydrophobicity of the sample. In this case, however, interpretation is difficult because system peaks corresponding to different concentration zones may additionally be present. This may be an indication that many components in the sample are associated to others through weak bonds (H, π, metal bridges) and that these bonds can interact and compete with the SDS micelles.

Fulvic acids generally show higher polydispersity (wider peaks) than humic acids. Several separated sharp peaks, corresponding to lower-molecular-mass compounds, were often found in the fulvic acid fractions and rarely in the humic acid mixtures. Some of the sharp peaks rising out of the humps were identified as phenolic acids such as syringic (a), vanillic (b) and *p*-hydroxybenzoic (c) acids by spiking the fulvic samples and comparing the UV spectra [80]. The presence of such low-molecular-mass acids in the humic mixture was previously demonstrated with ^{1}H-nuclear magnetic resonance (NMR) spectroscopy [81] and recently with capillary electrochromatography combined with two-dimensional NMR techniques [82]. These phenolic acids could have been released in solution by partial hydrolysis of the fulvic acid core or/and coextracted from the natural soil matrix; they ultimately result from the oxidation of lignin structures (soft or hard wood origins) and are found in different amounts characteristic of the vegetation of the studied soils [83]. This low-molecular-mass fraction, which can account for up to 30% of the dissolved organic carbon of the FA mixture (less than 5 to 10% in humic acids), can be nicely separated with CZE into single molecular peaks (molecular behavior) as compared to the humic hump (colloidal behavior) [62,84]. Studies are still in progress for the structural identification of these ionized hydroxycarboxylates with CE–electrospray ionization (ESI) MS [78].

Fig. 3 shows a typical example of two ultrafiltration fractions from a white water Amazon river site (Duke). The average mobility at 3 different pH are not significantly different when comparing the high (>10 000) and low (1000<<10 000) molecular mass leachates, and in both sample single peaks corresponding to low-molecular-mass substances are present. The fraction (1000<<10 000) additionally shows a more pronounced *double-hump* and a shoulder in the low mobility area present at pH 9.3 and 11.4 due to low-molecular-mass phenolic substances (not ionized at pH 5). This example also reveals that signals in the low mobility area are not necessary of

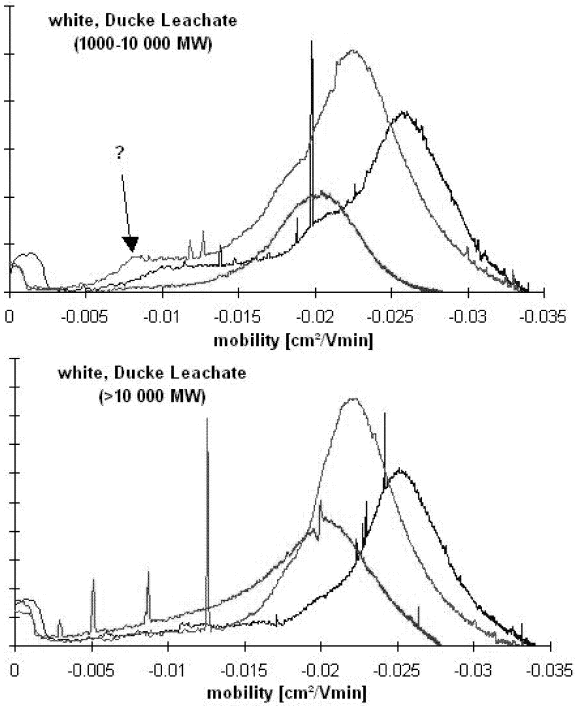

Fig. 3. CZE of ultra-filtrated dissolved organic matter obtained from the Amazon basin (Dr. A. Aufdencampe/Professor J. Hedges, University of Washington, USA). (The peak maxima of the mobility distribution from left to right correspond to separation buffer at pH 5, pH 9.3, pH 11.4).

high molecular mass, as has been expressed a few times in the literature on CE of HSs. Only a mass-selective detector (mass spectrometer) makes the differentiation of the charge and mass distributions within the polydisperse humic mixtures possible [85].

4. What experimental parameter can influence the shape of the electropherograms?

4.1. Local sample concentrations in the capillary due to injection and separation conditions

For a given sample load, the local concentration of

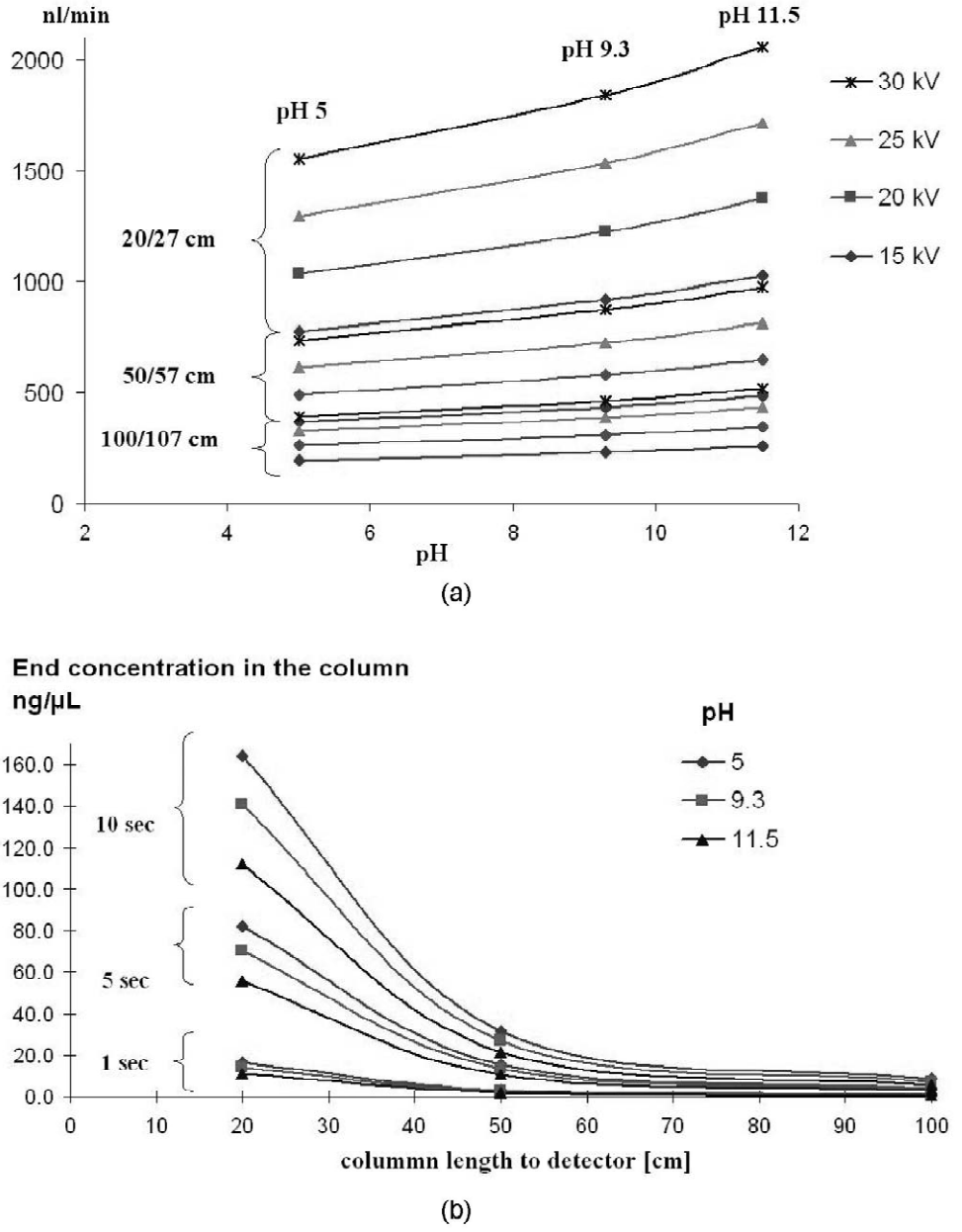

Fig. 4. (a) Dependence of the buffer flow velocity on experimental parameters; (b) average concentration of HSs in the capillary at the detector for different injection times and buffer pH (consequently different EOF), starting with a 2 mg/ml sample.

the sample in the capillary during the separation process is a function of its initial concentration and of the dilution during separation. The last effect is directly related to the volume of buffer that passes the detector during the time of measurement and is thus proportional to the EOF, the applied voltage and the capillary length.

Voltages from a few kV up to a maximum of 30 kV can be applied to the electrodes across the capillary loaded with separation buffer and the sample. Separation efficiency, endoosmotic flow, and thus analysis time are dependent on the voltage and the capillary length (field strength in V/cm). This is illustrated by the two figures ahead. The flow in the capillary (due to the pH-dependent EOF) is dependent on the field strength and thus on the capillary lengths (27 to 107 cm) and the voltage (15 to 30 kV); flow velocities between 200 nl/min and

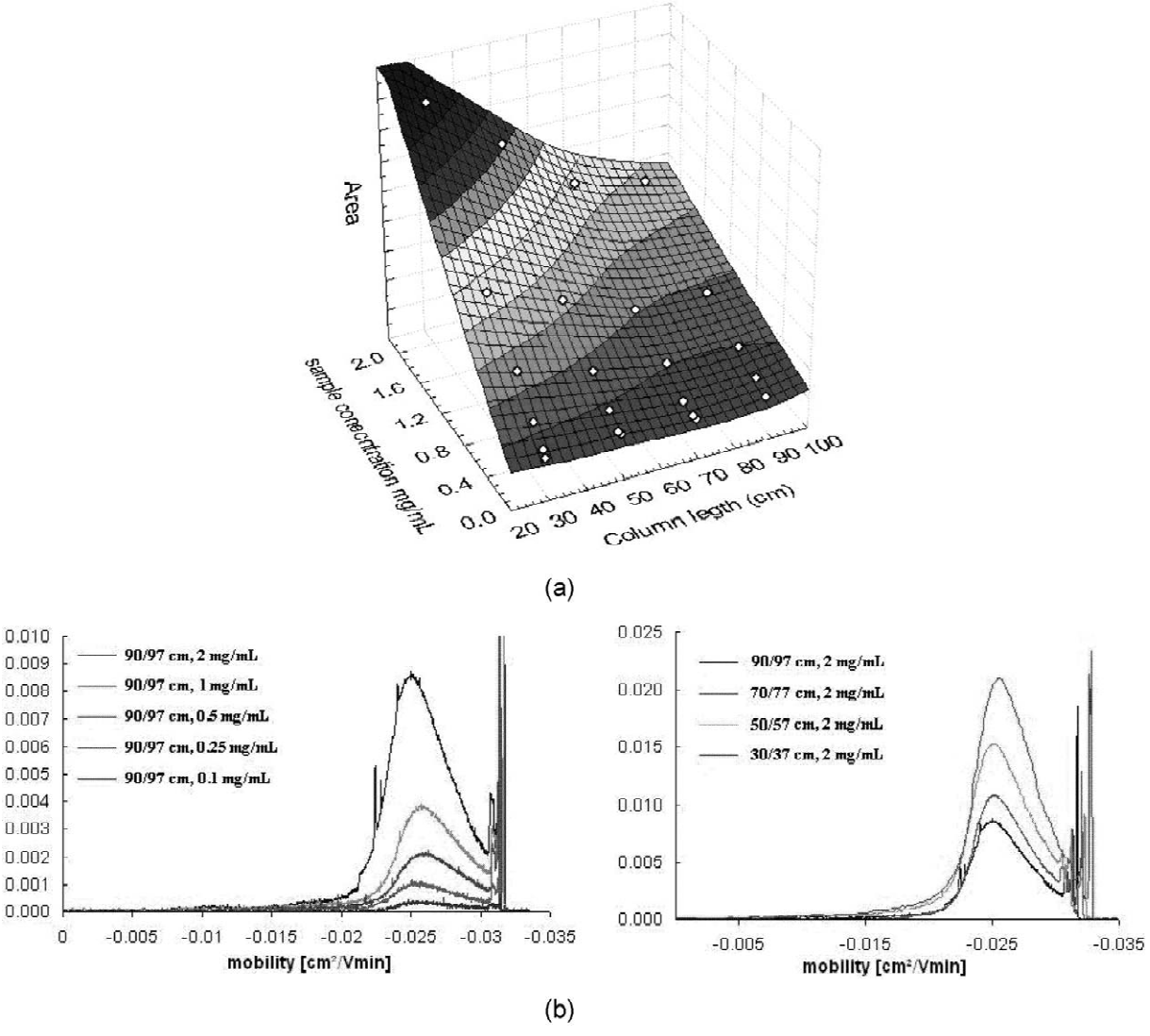

Fig. 5. (a) Linear relation between the signal intensity and the injected sample amount (sample concentration and column length effect); electropherogram by varying (b) sample concentration and (c) column length. Local concentration changes in the capillary have no effect on the mobility distribution.

2 μl/min can be obtained in the pH range from 5 to 11.5 (Fig. 4a).

When injecting a mixture of substances polydisperse in charge and/or in size (such as NOM), the obtained signals show a distribution in the effective mobility. The corresponding time window is dependent on the column length and the applied voltage. The velocity of the buffer will govern the residence time and thus the dilution of the sample during its passage in the capillary towards the detector. Fig. 4b illustrates this dilution effect using the flows from Fig. 4a as a function of pH, column voltage and injection time; the average end concentration in the column is given for a start solution of 2 mg/ml and a capillary of 75 μm I.D.

Although sample concentration needs to be high enough to get an interpretable signal, the dilution effect in this setup leads to an average concentration in the capillary of around 20 mg/l (dilution 100) with a 57 cm (50 cm effective length) column and 5 s injection (0.5 p.s.i.; 1 p.s.i.=6894.76 Pa). Because the signal distribution is Gaussian, local concentrations of over double the concentrations shown in Fig. 4b can be reached.

Due to the contribution of the sample to the local ionic strength, zones of different concentration could behave in the capillary as zones of different ionic strength with consequently different field strengths that influence the ion mobility (higher ion mobility in lower-ionic-strength regions). These could in some extreme cases (too low buffer ionic strength, short capillary) lead to field distortions and system peak formations (signals due to relative accumulation or depletion of ions within the mobility distribution zone). Such phenomena were also observed in free flow electrophoresis (FFE) experiments [86].

4.2. Is the mobility distribution a function of the local sample concentration?

To induce different local concentrations in the capillary, we tested different capillary lengths (from 37 to 97 cm) loaded with different sample concentrations (from 0.1 to 2 mg/ml). The injection times were chosen to always load the capillary with 60 nl of sample. The use of a short 27 cm column caused peak distortions and was not included in the comparison.

A linear response of the integrated peak signals relative to concentration was found for all investigated capillary lengths (Fig. 5a). For identical sample concentrations, the short capillary showed the highest integration signals (shorter analysis time and thus higher local sample concentration). In all measurements illustrated in Fig. 5b–c the mobility distribution was not significantly different, showing that the local sample concentration in the capillary did not affect the mobility distribution. Some authors [34] interpreted changes in the electrophoretic patterns as oligomerization/aggregation of humic substances, comparing electropherograms in the time scale without taking into account the drastic changes in migration time due to the change in EOF. This shows that lot of care has to be taken when interpreting CE data to avoid misinterpretation of electropherograms.

5. Causes of artifact peaks

The presence of sharp peaks in the high mobility region is dependent on separation conditions (voltage, column length, buffer velocity—ionic strength). To investigate these secondary effects, a buffer system (carbonate buffers) was chosen where only little or no interactions between buffer constituents and sample are to be expected.

5.1. Possible pitfalls caused by interactions with buffer constituents

HSs are well known to interact with organic and inorganic components and many studies have confirmed the relations between active humic binding sites and their specific reactivity toward selected chemicals [87,88]. Affinity capillary electrophoresis is actually used to study analyte–ligand interactions between all types of components. This is done by systematically increasing the concentration of the ligand in the CE background buffer and injecting the analyte as sample—it looks like an ordinary CE separation, only that the mobility of the analyte is a weighted function of the mobility of the free and bound analyte. Different 1:1 interaction models or partitioning models can then be applied to extract interaction information from series of electrophero-

grams. We have used this method repeatedly to analyze the binding to HSs of cationic *s*-triiazines [89], zwitterionic fluoroquinolones [90], anionic phenoxy acids of neutral hydrophobic polyaromatic hydrocarbons, and metals [91]. Detailed understanding of the interaction of *s*-triiazines with SDS micelles could also be followed that way [92]. The method allows the measurement of fast exchange interactions. The combination of many different analytes in one run makes a rapid investigation of different ligands possible and allows a quantitative structure–activity relation (QSAR) approach [93].

Fig. 6 illustrates these ACE principles taking as example the interaction of pyrene with a selected humic acid: the mobility of the complex is the average mobility of the humic acid, and by using a partitioning model the log K_{oc} (binding constant normalized to organic carbon content) obtained is 4.11, that is in the range of literature values [94,95]. This illustrates also the phenomenon of solubility enhancement [96] that lead to the membrane or micellar concepts of humic substances presented by Wershaw [97,98].

Due to the nature of the humic samples (polydisperse, heterogeneous, reactive), possible interferences with the buffer constituents are highly probable and can only be minimized, but hardly fully avoided. Due to the anionic structure characteristics of the HSs it becomes clear that any type of cationic buffer will be able to interact with some fractions of the HSs to some extent! This is also true for other

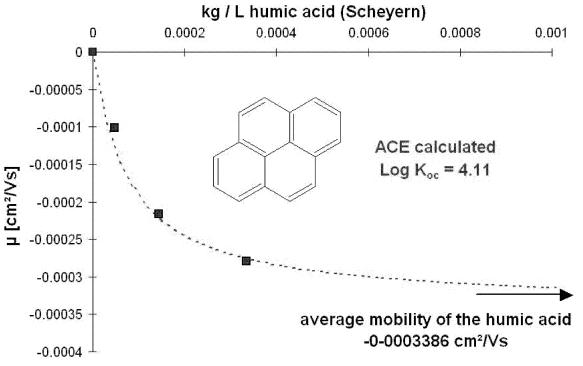

Fig. 6. Affinity capillary electrophoresis study of the binding of pyrene to natural organic matter (Scheyern, brown soil humic acid); pyrene was detected with laser-induced fluorescence (LIF, λ_{ex} 325 nm).

zwitterionic, so called ‘‘good buffers’’ [Tris, 4-(2-hydroxyethyl)-1-piperazineethanesulfonic acid (HEPES), MOBS (4-(*N*-Morpholino)butanesulfonic acid), etc.], that are chemically similar to the amphoteric ampholytes used in isoelectric focusing (IEF). The latter were shown to interact strongly with HSs [77,84].

These complexing buffers may be used to fingerprint NO*M*, but no structural interpretation should be made. The influence of tetrahydroxyborate ions on the electrophoretic mobility of humic acids was already proposed in 1995 [37] and systematically evaluated by CE in following studies [66,80]. Depending on the molarity of borate ions in the separation buffer, the humic acids exhibit electropherograms with sharp peaks consistently extending from a ‘‘humic hump’’. Variations in the migration times of these peaks depend on the concentration of borate ions in the separation buffer. The complexation of borate ions and humic acid fractions was also analyzed with ^{11}B- and ^{1}H-NMR spectroscopy as well as UV spectrophotometry in solutions of the same composition as the CE separation buffers. Supplementary studies with model compounds (flavonoids, phenolic and sugar acids) [99] indicate reaction mechanisms that include the formation of bidentate esters (monocomplexes) as well as spiranes (tetradentate esters or dicomplexes) within the humic substructure.

It was thus shown that special attention must be given to the interpretation of CE electropherograms while fingerprinting humic substances with borate buffers since observed peaks do not necessarily indicate distinct humic components but may be artifacts (that can also be used for fingerprinting purposes) caused by the interaction of the buffer ions with the humic substances.

To avoid system peaks due to different ionic strengths distributions within the capillary, extreme situations should be excluded. We systematically tried to keep the ionic strength of the buffers at 25 m*M*, and always tried to measure with voltages between 20 and 30 kV [capillary of 57 cm (50 cm effective length)×75 μm I.D.]. Only acetate and carbonate buffers were used, which were in these terms non-interacting with the sample. In these conditions system peaks were limited. In contrast to many studies stating that small acids (i.e., acetic

acid) are able to disrupt supramolecular complexes of humic substances [100–104], we were never able to observe such a phenomenon. Because of possible surface interactions [105] and colloidal properties of NOM [106], it is strongly believed that many artifacts can additionally lead to biased results in high-performance size-exclusion chromatography (HPSEC) when system parameters are not properly checked and interpreted [107,108].

5.2. Possible operational pitfalls caused by experimental setup

Sharp system peaks need to be differentiated from signals caused by the interaction with buffer components. Very often both types of signals can be superimposed on the samples' own electrophoretic pattern. Peak distortion was already observed when analyzing liposome preparations with CZE [109] and was expected to come from peculiar electric processes occurring at the boundary of the initial sample zone and the background electrolyte. Because humic substances and NOM are anionic in nature, they can contribute to the local ionic strength distribution in the capillary during their separation. This can cause field strength gradients within the capillary that can cause moving zones or unwanted zone concentration (staking) effects. Using free flow electrophoresis it was shown that within the humic hump pH differences of up to 0.5 pH units can occur [86].

We systematically changed separation parameters and looked at the effects on the presence and evolution of such system peaks. The chosen sample was the Suwannee River NOM (SRNOM) at a concentration of 1 mg/ml analyzed in a 57 cm (50 cm effective length) capillary column.

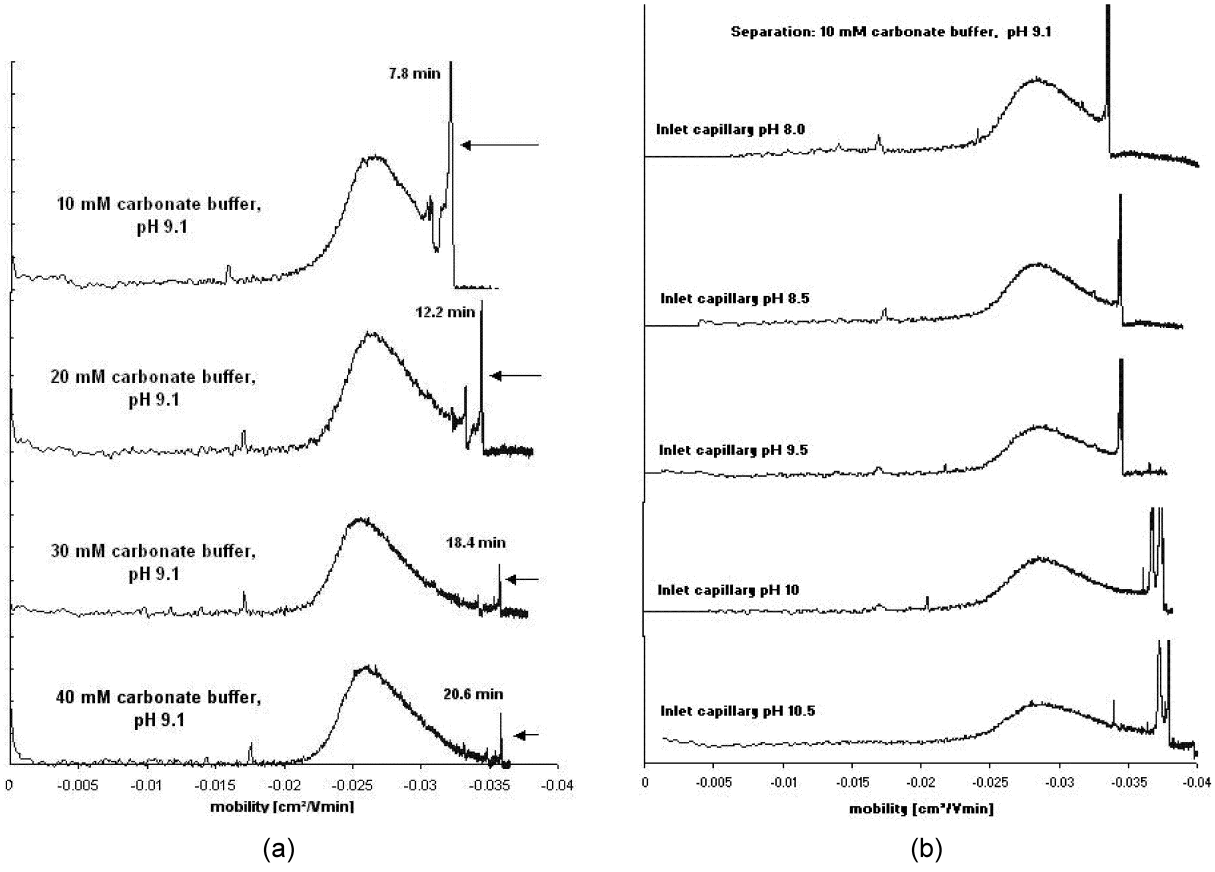

Fig. 7. (a) Ionic strength and (b) pH effects on peak compression.

5.2.1. Ionic strength

It was observed that lower buffer ionic strength favors peak formation. The signals show a sharp asymmetrical front coming from the high mobility side (high migration times) Fig. 7a. The lower the molarity of the buffer, the more the zone is focused and the higher the formed peak becomes. The field strength is higher in low molarity buffers and so is the corresponding ion velocity. When these fast moving ions are approaching sample zones of higher local ionic strength and lower field strength (such as in the humic hump), they are slowed down and show staking effects (the same effect is used for concentration of charged analytes between buffer zones).

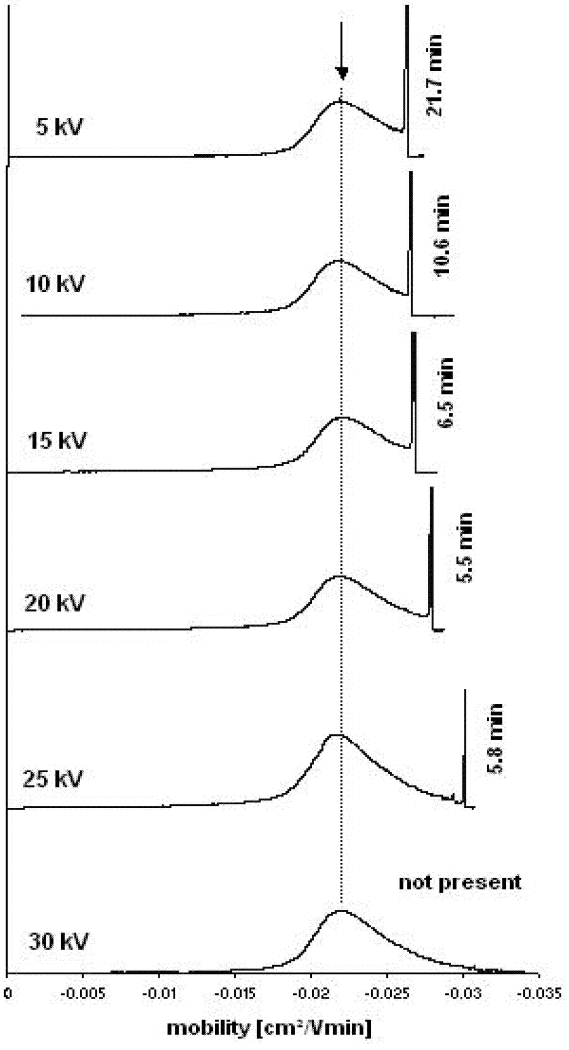

Fig. 8. Effect of voltage on NOM electropherograms.

5.2.2. Inlet pH effects

During the separation, ion depletion leads to a pH increase in the inlet reservoir and an acidification of the outlet reservoir. The higher the buffer molarity, the higher is its buffer capacity and the corresponding measurements can be done for a longer time before pH changes become significant.

We simulated that effect in the inlet vial. We filled the capillary with the same 10 m*M* carbonate buffer but changed the pH at the inlet electrode before starting the separation (Fig. 7b). Higher pH in the inlet vial favors stronger peak formation. This confirms also the ionic strength effects: a higher molarity buffer is less affected by changes in pH during the separation process (higher buffering effect) and thus contributes in lesser extent to these zone effects.

5.2.3. Voltage effects

Changing the separation voltage also showed systematic peak sharpening effects (Fig. 8). The lower the voltage, the more these effects take place. For the same buffer, longer separation time favor staking (with longer separation times the buffering action of the buffer in the inlet vial is decreasing).

6. Conclusion

CE is a versatile and powerful tool with a high separation efficiency and selectivity when analyzing mixtures of low-molecular-mass components. Many papers were published on the subject over the last years but unfortunately they often only give a limited image on the real possibilities of CE in the field of HSs. On the stony road to consistent results, not only the complexity, heterogeneity and polydispersity of humic substances may limit straightforward conclusions, but also many artifacts can result from the chosen separation buffer chemistry or from hidden instrumental constraints. We believe that CE and capillary electrochromatography approaches contribute to a better understanding of the solution behavior of HSs, especially when additionally combined (offline or online) with powerful spectrometric and

spectroscopic techniques such as multidimensional NMR [82] and mass spectrometry [71,85].

Acknowledgements

Thanks are due to H. Neumeir, A. Wüst, B. Look and B. Kopplin of the Institute for Ecological Chemistry—GSF, for skillful technical assistance. Part of this work was supported by the German–Israeli Foundation for Scientific Research and Development, GIF Young Scientist No. 2015-1084.08/2000.

References

[1] M.N. Jones, N.D. Bryan, Adv. Colloid Interface Sci. 78 (1998) 1.
[2] P.G. Hatcher, D.J. Clifford, Org. Geochem. 27 (1997) 251.
[3] P. Schmitt-Kopplin, N. Hertkorn, H.-R. Schulten, D. Freitag, A. Kettrup, Environ. Sci. Technol. 32 (1998) 89.
[4] N. Hertkorn, H. Claus, P. Schmitt-Kopplin, M.E. Perdue, Z. Filip, Environ. Sci. Technol. 36 (2002) 4334.
[5] A. Zsolnay, Dissolved Humus in Soil Waters, Elsevier, Amsterdam, 1996.
[6] J. Buffle, Complexation Reactions in Aquatic Systems, Ellis Horwood, Chichester, 1988.
[7] P. Schmitt-Kopplin, I. Twardowska, J. Kyziol, D. Freitag, A. Kettrup, Org. Geochem., submitted for publication.
[8] P. Schmitt, Y. Sanlaville, J. Lintelmann, D. Freitag, A. Kettrup, J. Chromatogr. A 709 (1995) 215.
[9] J.I. Hedges, J.M. Oades, Org. Geochem. 21 (1997) 319.
[10] G.R. Aiken, Humic Substances in Soil, Sediment, And Water, Wiley, New York, 1985.
[11] J.A. Leenheer, R.L. Wershaw, M.M. Reddy, Environ. Sci. Technol. 29 (1995) 393.
[12] J.A. Leenheer, R.L. Wershaw, M.M. Reddy, Environ. Sci. Technol. 29 (1995) 399.
[13] S.M. Shevchenko, G.W. Bailey, Crit. Rev. Environ. Sci. Technol. 26 (1996) 95.
[14] J.R. Lead, W. Davison, J. Hamilton-Taylor, J. Buffle, Aquat. Geochem. 3 (1997) 213.
[15] S.E. Cabaniss, Q. Zhou, P.A. Maurice, Y.-P. Chin, G.R. Aiken, Environ. Sci. Technol. 34 (2000) 1103.
[16] R.A. Neihof, G.I. Loeb, Limnol. Oceanogr. 17 (1972) 7.
[17] R.A. Neihof, G.I. Loeb, J. Marine Res. 32 (1973) 5.
[18] K.A. Hunter, Limnol. Oceanogr. 25 (1980) 807.
[19] G. Bragato, A. Mori, M. De Nobili, Eur. J. Soil Sci. 49 (1998) 589.
[20] S.B. Ceppi, M.I. Velasco, D. Fetsch, J. Havel, Bol. Soc. Chil. Quim. 44 (1999) 401.
[21] C. Ciavatta, M. Govi, L. Sitti, C. Gessa, Commun. Soil Sci. Plant Anal. 26 (1995) 3305.
[22] C. Ciavatta, M. Govi, C. Gessa, J. High Resolut. Chromatogr. 20 (1997) 67.
[23] J. Dahlén, B. Allard, H. Borén, in: J. Drozd, S.S. Gonet, N. Senesi, J. Weber (Eds.), The Role of Humic Substances in the Ecosystems and in Environmental Protection, Polish Society of Humic Substances, Wroclaw, 1997, p. 533.
[24] M. De Nobili, F. Fornasier, G. Bragato, in: J. Drozd, S.S. Gonet, N. Senesi, J. Weber (Eds.), The Role of Humic Substances in the Ecosystems and in Environmental Protection, Polish Society of Humic Substances, Wroclaw, 1997, p. 97.
[25] M. De Nobili, G. Bragato, A. Mori, Acta Hydrochim. Hydrobiol. 26 (1998) 186.
[26] M. De Nobili, G. Bragato, A. Mori, in: G. Davies, E. Ghabbour, K. Khairy (Eds.), Humic Substances: Structures, Properties and Uses, Royal Society of Chemistry, Cambridge, 1998, p. 109.
[27] M. De Nobili, G. Bragato, A. Mori, J. Chromatogr. A 863 (1999) 195.
[28] M. De Nobili, G. Bragato, A. Mori, in: E. Ghabbour, G. Davies (Eds.), Humic Substances: Structures, Models and Functions, Royal Society of Chemistry, Cambridge, 2001, p. 109.
[29] M. De Nobili, G. Bragato, A. Mori, in: R. Swift, K. Spark (Eds.), Understanding and Managing Organic Matter in Soils, Sediments, And Waters, International Humic Substances Society, St. Paul, MN, 2001, p. 91.
[30] R. Dunkel, H.-H. Rüttinger, K. Peisker, J. Chromatogr. A 777 (1997) 335.
[31] P.K. Egeberg, S.O. Bergli, J. Chromatogr. A 950 (2002) 221.
[32] D. Fetsch, M. Fetsch, E.M. Pena Mendéz, J. Havel, Electrophoresis 19 (1998) 2465.
[33] D. Fetsch, J. Havel, J. Chromatogr. A 802 (1998) 189.
[34] D. Fetsch, M. Hradilová, E.M. Pena Méndez, J. Havel, J. Chromatogr. A 817 (1998) 313.
[35] D. Gajdosová, L. Pokorná, A. Kotz, J. Havel, in: E. Ghabbour, G. Davies (Eds.), Humic Substances—Versatile Components of Plants, Soil and Water, Royal Society of Chemistry, Cambridge, 2000, p. 289.
[36] D. Gajdosová, L. Pokorná, P. Prosek, K. Láska, J. Havel, in: E. Ghabbour, G. Davies (Eds.), Humic Substances: Structures, Models and Functions, Royal Society of Chemistry, Cambridge, 2001, p. 121.
[37] A.W. Garrison, P. Schmitt, A. Kettrup, Water Res. 29 (1995) 2149.
[38] J. Havel, D. Fetsch, E. Pena Mendéz, P. Lubal, J. Havlis, in: R. Swift, K. Spark (Eds.), Understanding and Managing Organic Matter in Soils, Sediments, And Waters, International Humic Substances Society, St. Paul, MN, 2001, p. 77.
[39] M. Hosse, K.J. Wilkinson, Environ. Sci. Technol. 35 (2001) 4301.
[40] P. Schmitt-Kopplin, Environ. Sci. Technol. 36 (2002) 3041.
[41] D. Kaniansky, V. Zelenská, M. Masár, F. Iványi, S. Gazdikova, J. Chromatogr. A 844 (1999) 349.
[42] P. Kopácek, D. Kaniansky, J. Hejzlar, J. Chromatogr. 545 (1991) 461.

[43] Z. Krivácsy, G. Kiss, B. Varga, I. Galambos, Z. Sárvári, A. Gelencsér, Á. Molnár, S. Fuzzi, M.C. Facchini, S. Zappoli, A. Andracchio, T. Alsberg, H.C. Hansson, L. Persson, Atmos. Environ. 34 (2000) 4273.
[44] M.D. Landgraf, R.C.A. Javaroni, M.O.O. Rezende, J. Cap. Electrophoresis 5 (1998) 193.
[45] M. Nordén, E. Dabek-Zlotorzynska, J. Chromatogr. A 739 (1996) 421.
[46] M. Nordén, E. Dabek-Zlotorzynska, Electrophoresis 18 (1997) 292.
[47] M.L. Pacheco, J. Havel, Electrophoresis 23 (2002) 268.
[48] E. Parlanti, B. Morin, L. Vacher, Org. Geochem. 33 (2002) 221.
[49] L. Pokorná, D. Gajdosová, S. Mikeska, J. Havel, in: E. Ghabbour, G. Davies (Eds.), Humic Substances—Versatile Components of Plants, Soil and Water, Royal Society of Chemistry, Cambridge, 2000, p. 299.
[50] L. Pokorná, M.L. Pacheco, J. Havel, J. Chromatogr. A 895 (2000) 345.
[51] L. Pokorná, D. Gajdosová, S. Mikeska, P. Homolác, J. Havel, in: E. Ghabbour, G. Davies (Eds.), Humic Substances: Structures, Models and Functions, Royal Society of Chemistry, Cambridge, 2001, p. 133.
[52] S. Pompe, M. Bubner, M.A. Denecke, T. Reich, A. Brachmann, G. Geipel, R. Nicolai, K.H. Heise, H. Nitsche, Radiochim. Acta 74 (1996) 135.
[53] S. Pompe, K.-H. Heise, H. Nitsche, J. Chromatogr. A 723 (1996) 215.
[54] A. Rigol, J.F. López-Sánchez, G. Rauret, Quim. Anal. 13 (1994) 11.
[55] A. Rigol, J.F. López-Sánchez, G. Rauret, J. Chromatogr. A 664 (1994) 301.
[56] A. Rigol, M. Vidal, G. Rauret, J. Radioanal. Nucl. Chem. 208 (1996) 617.
[57] A. Rigol, M. Vidal, G. Rauret, J. Chromatogr. A 807 (1998) 275.
[58] P. Schmitt, A. Kettrup, GIT Fachz. Lab. 12 (1994) 1310.
[59] P. Schmitt, D. Freitag, Y. Sanlaville, J. Lintelmann, A. Kettrup, J. Chromatogr. A 709 (1995) 215.
[60] P. Schmitt, A. Kettrup, D. Freitag, A.W. Garrison, Fresenius J. Anal. Chem. 354 (1996) 915.
[61] P. Schmitt, D. Freitag, I. Trapp, A.W. Garrison, M. Schiavon, A. Kettrup, Chemosphere 35 (1997) 55.
[62] P. Schmitt, A.W. Garrison, D. Freitag, A. Kettrup, Water Res. 31 (1997) 2037.
[63] P. Schmitt, N. Hertkorn, A. Hoppe, A.W. Garrison, D. Freitag, A. Kettrup, in: J. Drozd, S.S. Gonet, N. Senesi, J. Weber (Eds.), The Role of Humic Substances in the Ecosystems and in Environmental Protection, Polish Society of Humic Substances, Wroclaw, 1997.
[64] P. Schmitt-Kopplin, A.W. Garrison, E.M. Perdue, D. Freitag, A. Kettrup, J. Chromatogr. A 807 (1998) 101.
[65] P. Schmitt-Kopplin, N. Hertkorn, H.-R. Schulten, A. Kettrup, Environ. Sci. Technol. 32 (1998) 2531.
[66] P. Schmitt-Kopplin, N. Hertkorn, A.W. Garrison, D. Freitag, A. Kettrup, Anal. Chem. 70 (1998) 3798.
[67] P. Schmitt-Kopplin, J. Burhenne, D. Freitag, M. Spiteller, A. Kettrup, J. Chromatogr. A 837 (1999) 253.
[68] P. Schmitt-Kopplin, D. Freitag, A. Kettrup, N. Hertkorn, U. Schoen, R. Klöckling, B. Helbig, F. Andreux, A.W. Garrison, Analusis 27 (1999) 390.
[69] P. Schmitt-Kopplin, N. Hertkorn, D. Freitag, A. Kettrup, A.V. Garmash, A.V. Kudryavtsev, I. Perminova, V.S. Pertosyan, J. AOAC Int. 82 (1999) 1594.
[70] P. Schmitt-Kopplin, U. Schoen, P.K. Egeberg, D. Freitag, A. Kettrup, Environ. Int. 25 (1999) 259.
[71] P. Schmitt-Kopplin, in: Habilitationschrift, Wissenschaftszentrum Weihenstephan für Ernährung, Landnutzung und Umwelt, TUM, Munich-Weihenstephan, 2002, p. 250.
[72] J.J. van Staden, M.A.G.T. van den Hoop, R.F.M.J. Cleven, in: Characterisation of metal/humic acid systems through capillary electrophoresis, National Institute of Public Health and the Environment, Bilthoven, 2000, p. 1.
[73] S. Wakida, X. Wu, A. Chiba, T. Matsuda, H. Nakanishi, S. Kurosawa, H. Nagai, K. Fukushi, S. Takeda, Anal. Sci. 17 (2001) 445.
[74] C. Wang, A. Peng, P. Schmitt, N. Hertkorn, Acta Scient. Circumst. 16 (1996) 270.
[75] P. Barak, Y. Chen, Soil Sci. 154 (1992) 184.
[76] P. Schmitt-Kopplin, D. Freitag, A. Kettrup, N. Hertkorn, U. Schoen, R. Klöcking, B. Helbig, F. Andreux, A.W. Garrison, Analusis 27 (1999) 6.
[77] P. Schmitt-Kopplin, D. Freitag, A. Kettrup, U. Schoen, P. Egeberg, Environ. Int. 25 (1999) 259.
[78] P. Schmitt-Kopplin, F. Menzinger, D. Freitag, A. Kettrup, LC·GC Eur. 14 (2001) 284.
[79] P. Schmitt-Kopplin, A.V. Garmash, A.V. Kudryavtsev, F. Menzinger, I.V. Perminova, N. Hertkorn, D. Freitag, V.S. Petrosyan, A. Kettrup, Electrophoresis 22 (2001) 77.
[80] P. Schmitt-Kopplin, A.W. Garrison, E.M. Perdue, D. Freitag, A. Kettrup, J. Chromatogr. A 807 (1998) 101.
[81] M.A. Wilson, P.J. Collin, R.L. Malcom, E.M. Perdue, P. Cresswell, Org. Geochem. 12 (1988) 7.
[82] G. Ping, P. Schmitt-Kopplin, N. Hertkorn, W. Zhang, Y. Zhang, A. Kettrup, Electrophoresis 24 (2003) 958.
[83] O. Manan, F. Marseille, B. Guillet, J.R. Disnar, P. Morin, J. Chromatogr. A 755 (1996) 89.
[84] U. Schoen, in: Geowissenschaften, Katholische Universität Eichstätt, Eichstätt, 1999, p. 235.
[85] P. Schmitt-Kopplin, in: E.A. Ghabbour, G. Davies (Eds.), Humic Substances: Nature's Most Versatile Materials, Taylor and Francis, New York, 2003.
[86] J. Junkers, P. Schmitt-Kopplin, J.C. Munch, A. Kettrup, Electrophoresis 23 (2002) 2872.
[87] C.E.W. Steinberg, M. Haitzer, R. Brüggemann, I.V. Perminova, N.Y. Yashchenko, V.S. Petrosyan, Int. Rev. Hydrobiol. 85 (2000) 253.
[88] J. Peuravuori, Anal. Chim. Acta 429 (2001) 75.
[89] P. Schmitt, I. Trapp, A.W. Garrison, D. Freitag, A. Kettrup, Chemosphere 35 (1997) 55.
[90] P. Schmitt-Kopplin, J. Burhenne, D. Freitag, M. Spiteller, A. Kettrup, J. Chromatogr. A 837 (1999) 253.
[91] P. Schmitt, A.W. Garrison, D. Freitag, A. Kettrup, Fresenius J. Anal. Chem. 354 (1996) 915.
[92] D. Freitag, P. Schmitt-Kopplin, R. Simon, A. Kaune, A. Kettrup, Electrophoresis 20 (1999) 1568.

[93] P. Schmitt-Kopplin, D. Freitag, A. Kettrup, Interactions Entre *s*-Triazines et Substances Humique Dissoutes; les Potentialités de l'Électrophorèse Capillaire, BRGM, Orléans, 1997.
[94] Y.-P. Chin, G.R. Aiken, K.M. Danielsen, Environ. Sci. Technol. 31 (1997) 1630.
[95] C.T. Chiou, S.E. McGroddy, D.E. Kile, Environ. Sci. Technol. 32 (1998) 264.
[96] C.T. Chiou, D.E. Kile, T.I. Brinton, M. Malcom, J.A. Leenheer, P. MacCarthy, Environ. Sci. Technol. 21 (1987) 1231.
[97] R.L. Wershaw, J. Contam. Hydrol. 1 (1986).
[98] R.L. Wershaw, Environ. Health Perspect. 83 (1998) 191.
[99] P. Schmitt-Kopplin, K. Fischer, D. Freitag, A. Kettrup, J. Chromatogr. A 807 (1998) 89.
[100] P. Conte, A. Piccolo, Chemosphere 38 (1999) 517.
[101] A. Piccolo, P. Conte, A. Cozzolino, Soil Sci. 166 (2001) 174.
[102] A. Piccolo, S. Nardi, G. Concheri, Eur. J. Soil Sci. 47 (1996) 319.
[103] A. Piccolo, S. Nardi, G. Concheri, Chemosphere 33 (1996) 595.
[104] A. Piccolo, P. Conte, B. Lagen van, P. Buurman, Environ. Sci. Technol. 36 (2002) 76.
[105] I.V. Perminova, F.H. Frimmel, D.V. Kovalevskii, G. Abbt-Braun, A.V. Kudryavtsev, S. Hesse, Water Res. 32 (1998) 872.
[106] C.-H. Fischer, E. Kenndler, J. Chromatogr. A 773 (1997) 179.
[107] I.V. Perminova, Soil Sci. 164 (1999) 834.
[108] B. Varga, G. Kiss, I. Galambos, A. Gelencser, J. Hlavay, Z. Krivacsky, Environ. Sci. Technol. 34 (2000) 3303.
[109] S.P. Radko, M. Stastna, A. Chrambach, J. Chromatogr. B 761 (2001) 69.